⌘ *Author's Choice*

THE JOURNAL OF BIOLOGICAL CHEMISTRY VOL. 288, NO. 9, pp. 6763–6776, March 1, 2013
Published in the U.S.A.

# The p40 Subunit of Interleukin (IL)-12 Promotes Stabilization and Export of the p35 Subunit

## *IMPLICATIONS FOR IMPROVED IL-12 CYTOKINE PRODUCTION**

Received for publication, November 16, 2012, and in revised form, December 27, 2012 Published, JBC Papers in Press, January 7, 2013, DOI 10.1074/jbc.M112.436675

**Rashmi Jalah[‡], Margherita Rosati[§], Brunda Ganneru[§], Guy R. Pilkington[‡], Antonio Valentin[§], Viraj Kulkarni[‡], Cristina Bergamaschi[§], Bhabadeb Chowdhury[§], Gen-Mu Zhang[‡§], Rachel Kelly Beach[‡§], Candido Alicea[‡], Kate E. Broderick[¶], Niranjan Y. Sardesai[¶], George N. Pavlakis[§], and Barbara K. Felber[‡1]**

*From the [‡]Human Retrovirus Pathogenesis Section and [§]Human Retrovirus Section, Vaccine Branch, Center for Cancer Research, Frederick National Laboratory for Cancer Research, Frederick, Maryland 21702-1201 and [¶]Inovio Pharmaceuticals, Inc., Blue Bell, Pennsylania 19422-2200*

**Background:** The biosynthesis of IL-12p70 depends on the intracellular interaction of its p35 and p40 subunits.
**Results:** The p40 subunit stabilizes p35 and promotes its secretion.
**Conclusion:** Understanding the regulatory steps of IL-12 biosynthesis led to the generation of optimized IL-12 plasmids.
**Significance:** Availability of expression-optimized IL-12 DNA plasmids is important for practical applications as DNA vaccine adjuvants and in cancer immunotherapy.

**IL-12 is a 70-kDa heterodimeric cytokine composed of the p35 and p40 subunits. To maximize cytokine production from plasmid DNA, molecular steps controlling IL-12p70 biosynthesis at the posttranscriptional and posttranslational levels were investigated. We show that the combination of RNA/codon-optimized gene sequences and fine-tuning of the relative expression levels of the two subunits within a cell resulted in increased production of the IL-12p70 heterodimer. We found that the p40 subunit plays a critical role in enhancing the stability, intracellular trafficking, and export of the p35 subunit. This posttranslational regulation mediated by the p40 subunit is conserved in mammals. Based on these findings, dual gene expression vectors were generated, producing an optimal ratio of the two subunits, resulting in a ~1 log increase in human, rhesus, and murine IL-12p70 production compared with vectors expressing the wild type sequences. Such optimized DNA plasmids also produced significantly higher levels of systemic bioactive IL-12 upon *in vivo* DNA delivery in mice compared with plasmids expressing the wild type sequences. A single therapeutic injection of an optimized murine IL-12 DNA plasmid showed significantly more potent control of tumor development in the B16 melanoma cancer model in mice. Therefore, the improved IL-12p70 DNA vectors have promising potential for *in vivo* use as molecular vaccine adjuvants and in cancer immunotherapy.**

IL-12, initially described as "natural killer cell stimulatory factor" (1, 2), is a 70–75-kDa heterodimeric glycoprotein composed of two disulfide-linked subunits, p35 and p40. IL-12 is primarily produced by antigen-presenting cells and exerts immunoregulatory effects on natural killer and T cells. IL-12 plays a pivotal role in the initiation and maintenance of Th1 responses, especially in the induction of adaptive cellular immunity (for recent reviews, see Refs. 3–5 and references therein). Due to its immunomodulatory and anti-angiogenic properties, IL-12 has great potential as an efficient vaccine adjuvant and anticancer therapeutic agent (reviewed in Refs. 6–11)). In view of the central role of IL-12 in cell-mediated immunity, the mechanisms controlling its production and regulation are of great interest. Although co-expression of both subunits in the same cell is essential to form the biologically active heterodimer (12–14), production of each of the subunits is independently regulated. Regulation of expression of the p35 and the p40 genes has been studied in detail (reviewed in Refs. 4 and 15). The p35 gene is constitutively expressed in various cell types and tissues, whereas expression of p40 is restricted to cells producing IL-12. Unlike p35, the p40 subunit is secreted as monomer and homodimer (16, 17). Whereas most studies have focused on the activation of expression of IL-12p70, little is known about the direct effect of the different subunits on each other.

In this study, we addressed the molecular steps controlling the production of the heterodimeric IL-12p70 at the posttranscriptional level by studying the posttranslational fate of the individual subunits alone and in combination. This work was prompted by our findings on the critical intracellular regulatory steps that include cross-stabilization of the IL-15 chain and the so-called IL-15R$\alpha$,[2] which together form the circulating active heterodimeric IL-15 cytokine found in plasma (18–21). We investigated the interaction of the IL-12p35 and p40 subunits and found that p40 plays a critical role at the posttranslational level by stabilizing and promoting the transport of p35, which results in secretion of the heterodimeric IL-12p70. To better understand the biology of IL-12p70 and for potential use in

* This work was supported, in whole or in part, by the National Institutes of Health, NCI, Intramural Research Program.
⌘ *Author's Choice*—Final version full access.
[1] To whom correspondence should be addressed. Tel.: 301-846-5159; Fax: 301-846-7146; E-mail: felberb@mail.nih.gov.

[2] The abbreviations used are: IL-15R$\alpha$, IL-15 receptor $\alpha$; huCMV and siCMV, human and simian cytomegalovirus, respectively; CHX, cycloheximide; nt, nucleotides; Endo F and Endo H, endoglycosidase F and H, respectively; ER, endoplasmic reticulum; TGN, trans-Golgi network; BisTris, 2-[bis(2-hydroxyethyl)amino]-2-(hydroxymethyl)propane-1,3-diol.

clinical applications, we generated optimized DNA plasmids producing high levels of IL-12 heterodimer for *in vivo* DNA delivery. We performed immunotherapeutic studies in mice using the B16 melanoma cancer model and found that the optimized murine IL-12p70 plasmid showed anticancer activity superior to that of a plasmid expressing the wild type IL-12 coding sequences. Thus, our studies on the basic mechanism governing the biosynthesis of IL-12 led to the development of improved plasmids for practical *in vivo* applications.

## EXPERIMENTAL PROCEDURES

*DNA Plasmids*—Dual promoter plasmids expressing the wild type human (plasmid WLV103M (22)), murine (plasmid WLV105 (23)) and rhesus macaque (plasmid WLV104M (24)) IL-12p70 from native coding sequences have been described. The protein sequences are identical to the sequences with the following GenBank™ accession numbers: human IL-12p35, P29459.2; human IL-12p40, NP_002178.2; rhesus IL-12p35, P48091.1; rhesus IL-12p40, NP_001038190.1; murine IL-12p35, NP_001152896; and murine IL-12p40, NP_032378. We designed RNA/codon-optimized coding sequences for the IL-12 p35 and p40 subunits following the principles described previously (25–27), and the genes were chemically synthesized and verified by nucleotide sequencing (GeneArt, Regensburg, Germany). These p35 and p40 sequences were cloned into single promoter (pCMVkan) and dual promotor (pDP, WLV-009M) eukaryotic expression plasmids. pCMVkan consists of the human cytomegalovirus (huCMV) promoter, an optimal surrounding for the AUG initiator codon from HIV-1 *tat* that prevents initiation of translation from internal AUGs, the bovine growth hormone polyadenylation signal, and the kanamycin resistance gene (*kan*) embedded in a plasmid backbone optimized for growth in bacteria, as described previously (27–30). The dual promoter vector pDP is derived from pCMVkan, consisting of the huCMV promoter linked to the bovine growth hormone polyadenylation signal and the weaker siCMV promoter linked to the SV40 pA site in counterclockwise orientation. Vector pWLV-009M contains the huCMV promoter linked to the SV40pA signal and the siCMV promoter linked to the bovine growth hormone polyadenylation signal in counterclockwise orientation (31). The pDP and pWLV-009M vectors differ in the plasmid backbone sequence and the kanamycin gene sequences. We noted that upon growth in bacteria, pDP-based plasmids have higher DNA yields.

The following RNA-optimized IL-12 cytokine plasmids were generated: (i) for human IL-12, the p35 (AG182), p40 (AG180), C-terminally 3× FLAG-tagged p35-FLAG (AG260) and p40-FLAG (AG261), IL-12p70 expressing p40 from the huCMV promoter and p35 from the siCMV promoter (AG181) or expressing p40 from the siCMV promoter and p35 from the huCMV promoter (AG183) from the DP expression vector, and IL-12p70 expressing p40 from the huCMV promoter (AG169) or siCMV promoter (AG5) from the WLV vector; (ii) for murine IL-12, p35 (AG248), p40 (AG247), and IL-12p70 expressing p40 from the huCMV promoter (AG250) from the DP expression vector; (iii) for rhesus macaque, rmIL-12p70 expressing p40 from the huCMV promoter (AG157) or siCMV promoter (AG159) from the DP expression vector or the WLV vector (AG167 and AG3, respectively). The optimized human p35 and p40 gene sequences share 75.9% (identity in 501 of 660 nt) and 75.7% (identity in 747 of 987 nt) with wild type sequences, respectively, and were used for plasmid AG180 and derivatives (AG181, AG182, and AG183). Another human IL-12 p70 plasmid (AG259) was generated with additional nt changes in both subunits (51 nt in p35 and 66 nt in p40).

*Expression of the IL-12 Subunits and Treatment of Cells*—Human HEK293 cells (seeded with $1 \times 10^6$ cells/60-mm plate) were transfected using the calcium phosphate coprecipitation technique. The next day, the cells were transfected with 100 ng of plasmids encoding IL-12p70 cytokine or the individual subunits using a total of 7 $\mu$g of DNA/plate, adjusted by Bluescript-derived pBSPL DNA. Cotransfection of 50 ng of the GFP plasmid pFRED143 (32) served as an internal control. After 6–15 h, the medium was changed, and the cells were harvested 48 h after transfection. Culture supernatants were collected, and cells were washed with PBS and lysed with three freeze-thaw cycles in 1 ml of 0.5× radioimmune precipitation assay buffer (Boston BioProducts, Ashland, MA) supplemented with protease inhibitor mixture tablets (Roche Applied Science). All transfections were performed with three independent clones or in duplicates. GFP levels of the cell extracts were measured using the SpectraMax Gemini EM fluorimeter (Molecular Devices, LLC, Sunnyvale, CA).

For tunicamycin treatment (Sigma-Aldrich), the medium was replaced with fresh medium at 1 day posttransfection, and 10–12 h later the medium was replaced with medium containing the inhibitor (10 $\mu$g/ml), and supernatants and cells were harvested 12–14 h posttreatment. For CHX treatment, the medium was replaced with fresh medium at 1 day posttransfection, and 3–4 h later, the medium was replaced with fresh medium containing 25 $\mu$g/ml CHX (Sigma-Aldrich). The cell-associated and extracellular fractions were collected at 0, 1, 2, and 4 h and analyzed on Western immunoblots. The bands were quantitated, and the accumulation of p35 and p40 when transfected alone or in combination was calculated over time by normalizing the value (sum of extracellular and cell-associated) at the start of the CHX treatment (time 0) as 100%. For endoglycosidase treatments, equal fractions of supernatants and cell lysates from transfected cells were digested for 1 h at 37 °C with endoglycosidase F (Endo F) or with endoglycosidase H (Endo H) (New England Biolabs, Inc., Ipswich, MA) following the manufacturer's instructions.

*Protein Analysis*—For Western immunoblot assays, aliquots (1/200) from the extracellular and cell-associated fractions were resolved on 12% NuPAGE Novex BisTris polyacrylamide gels using the NuPAGE MOPS SDS running buffer (Invitrogen). TGX Bio-Rad gels (4–15%) were used to analyze proteins under native conditions (no $\beta$-mercaptoethanol, no SDS), non-reducing conditions (treated with SDS, without $\beta$-mercaptoethanol), and reducing conditions (treated with $\beta$-mercaptoethanol and SDS). The membranes were probed with anti-IL-12 antibodies, followed by the anti-goat HRP secondary antibody (catalog no. 401504, Calbiochem). The polyclonal human IL-12p70 antibody (catalog no. AF219-NA; cross-reactive with rhesus IL-12p70), and the polyclonal murine IL-12p70 antibody (catalog no. AF419-NA, R&D Systems (Minneapolis,

MN)) were used. The FLAG-tagged proteins were detected by the monoclonal anti-FLAG M2-peroxidase (HRP) antibody (catalog no. A8592; Sigma-Aldrich). The bands were visualized using the ECL Plus Western blotting detection system (GE Healthcare) and imaged using autoradiography or the ChemiDoc™ XRS+ system from Bio-Rad. For quantification of bands, the Image Lab 3.0 software from Bio-Rad was used.

The IL-12p70 heterodimer production was quantitated using the human or murine IL-12p70 ELISA (catalog no. 88-7126 and catalog no. 88-7121, respectively, eBioscience (San Diego, CA)) or the rhesus macaque IL-12p70 ELISA (catalog no. KPC9121, Invitrogen). Mouse IFN-γ levels were measured by the "Femto-HS" High sensitivity ELISA (catalog no. 88-8314, eBioscience).

*Immunofluorescence*—The HeLa-derived HLtat cells (33) were plated with $2 \times 10^5$ cells/35-mm glass-bottomed plate and 24 h later were transfected with 200 ng of the human p35-FLAG (plasmid AG260), the human p40-FLAG (plasmid AG261), a mixture of 200 ng of p35-FLAG along with 600 ng of human p40 (plasmid AG180), or a mixture of 200 ng of p35 (plasmid AG182) along with 600 ng of human p40-FLAG. After 24 h, the cells were fixed with 4% paraformaldehyde in PBS, permeabilized with 0.5% Triton X-100 in PBS, and incubated with mouse anti-FLAG (Sigma) and rabbit anti-TGN46 (Novus Biologicals, Littleton, CO) antibodies (at 1:1000 dilution each), followed by incubation with anti-mouse Alexa-Fluor 488 and anti-rabbit Alexa-Fluor 594 (Invitrogen) secondary antibodies. Cells were visualized on a Zeiss Observer Z1 fluorescent microscope using Zeiss Axiovision software (Carl Zeiss Microimaging GmbH, Göttingen, Germany).

*DNA Delivery into Mice*—Female BALB/c and C57BL/6 (6–8 week old) mice were obtained from Charles River Laboratories, Inc. (Frederick, MD). The mice were housed at the Frederick National Laboratory for Cancer Research (Frederick, MD) in a temperature-controlled, light-cycled facility and were cared for under the guidelines of the Frederick National Laboratory Animal Care and Use Committee. Hydrodynamic DNA injection was performed in BALB/c mice as described previously (30, 34–36), using endotoxin-free preparation of DNA (Qiagen, Hilden, Germany). Briefly, cytokine DNA was suspended in 1.6 ml of sterile 0.9% NaCl and was injected into mice through their tail vein in a 7-s push, using a 27.5-gauge needle. For DNA injection via the intramuscular route, 5 μg of plasmid DNA in 50 μl of PBS was injected in the left and right quadriceps (25 μl/dose) followed by *in vivo* electroporation for DNA delivery using the ELGEN® adaptive constant current electroporation device (Inovio Pharmaceuticals, Inc., Blue Bell, PA).

*B16 Mouse Melanoma Model*—Groups of 8–10-week-old C57BL/6 mice ($n = 9$–12) were inoculated with $10^5$ B16 melanoma cells by intravenous injection. Two days later, the mice received the cytokine DNAs (5 and 50 ng/mouse, respectively) or sham DNA by hydrodynamic delivery. The mice were bled at day 1 post-cytokine DNA injection, and the IL-12p70 levels were measured from the plasma. After 3 weeks, mice were sacrificed, and the nodules in lungs were counted.

*Statistical Analysis*—Prism (version 4, GraphPad Software, Inc.) was used for all statistical analysis. Correlations were determined using the two-tailed nonparametric Spearman method. Comparison of different groups was done by one-way analysis of variance using Dunnett's multiple comparison test. Comparison between two experimental groups was performed using the nonparametric Mann-Whitney two-tailed *t* test at the 95% confidence interval.

## RESULTS

*The IL-12p40 Subunit Regulates the Trafficking and Export of the p35 Subunit*—To dissect steps in the biosynthesis of the IL-12p70 heterodimer, its p35 and p40 subunits were expressed independently from the CMV promoter using the mammalian expression vector pCMVkan, bypassing their natural transcriptional control. In addition to their AU-rich 3′-UTRs (12–14), we noted that the native p35 and p40 coding sequences have a relatively low AU content of ~50% and contain AU-rich segments, including AUUUA or AAUAA elements, which have been associated with low expression when present within the coding sequence, as we previously reported for HIV and SIV *gag* and *env* genes (25–27, 37), for IL-15 (30), and for the IL-15Rα (18, 19). To remove transcriptional and posttranscriptional impediments for IL-12p70 expression, the complete coding sequences of the human, macaque, or murine p35 and p40 were RNA- or codon-optimized (see "Experimental Procedures"). Production of optimized human p35 and p40 subunits was monitored upon transient transfection of HEK293 cells. Plasmids expressing FLAG-tagged human p35 and p40 were used to allow direct comparison of the production of respective subunits. Importantly, when expressed alone, the steady-state level of the p35 protein was much lower than that of p40 (Fig. 1*A*), both in the cell-associated and the extracellular fractions (compare *lanes 1* and *4 versus lanes 2* and *5*). A longer exposure was necessary to visualize both proteins; therefore, the p40 bands are overexposed. Most of the p35 subunit remained cell-associated, and the extracellular p35 migrated as diffuse bands due to different glycosylated forms (38, 39). In contrast, more p40 was found in the extracellular compartment. The steady-state protein levels and the localization changed when the two subunits were co-expressed in the same cell. We noted that the presence of p40 led to an overall increase in the total p35 protein level (Fig. 1*A*, compare *lanes 1* and *4* with *lanes 3* and *6*) as well as to a shift from p35 to increased accumulation in the extracellular compartment, suggesting that p40 affected not only the trafficking but also the stability (supported by pulse-chase experiments with CHX; see below) of the p35 subunit (Fig. 1*A*, compare *lanes 4* and *6*).

We further investigated the effect of p40 on the production and secretion of IL-12p70 using plasmids that express the untagged subunits (Fig. 1*B*). The cytokine production was analyzed by Western immunoblot assays from the intracellular and extracellular fractions with an IL-12p70 antibody recognizing both subunits, and the heterodimer production was quantified using an IL-12p70-specific ELISA. Upon expression of each subunit alone, results similar to those in Fig. 1*A* were obtained. Weak diffuse bands of p35 migrating at ~36 kDa (*lane 1*) were found in both compartments and readily detectable p40 migrating at ~40–43 kDa (*lane 2*) was found mostly in the extracellular compartment, as reported (16, 39). Upon cotransfection of equal amounts of plasmid DNAs expressing the

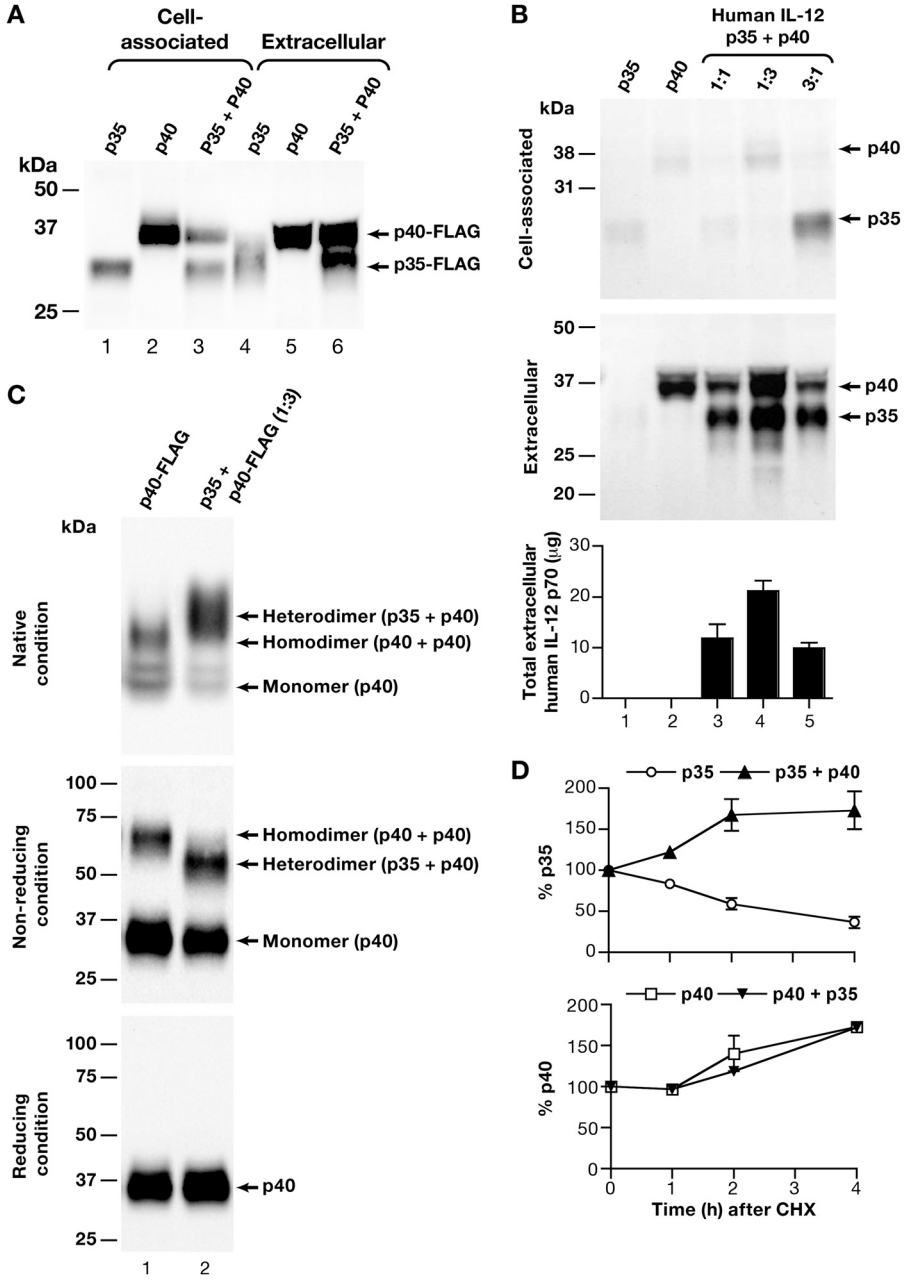


FIGURE 1. **Role of IL-12p40 in the production and secretion of the IL-12p70 heterodimer.** HEK293 cells were transfected with 100 ng of plasmids encoding the individual subunits alone, with a mixture of 100 ng each of the two plasmids together, or with a mixture of plasmids at the indicated ratios. Aliquots of the cell-associated and/or extracellular fraction were analyzed by Western immunoblot assays and by ELISA. The molecular mass standards (kDa) are indicated. Cotransfection of a GFP plasmid served as internal control. *A*, expression of the FLAG-tagged human IL-12p35 and IL-12p40 subunits alone (*lanes 1* and *2*) or together (*lane 3*) in the cell-associated (*lanes 1–3*) and extracellular (*lanes 4–6*) fraction. GFP values (mean ± S.E.) were 20.3 ± 6.0, 24.8 ± 2.4, and 17.5 ± 3.3 arbitrary units for *lanes 1–3*, respectively. A representative experiment is shown. *B*, optimization of co-expression of the untagged human IL-12p40 and IL-12p35 subunits expressed alone (*lanes 1* and *2*, respectively) or together using different DNA ratios as indicated (*lanes 3–5*). Analysis of the cell-associated (*top*) and extracellular fractions (*middle*) by Western immunoblot assays and by a human IL-12p70 specific ELISA (*bottom*) are shown. The mean of the values obtained from three independent and the S.E. (*error bars*) are shown. GFP values (mean ± S.E.) were 4.8 ± 0.7, 8.2 ± 0.9, 8.6 ± 2.1, 9.5 ± 1.5, and 8.4 ± 1.4 arbitrary units for *lanes 1–5*, respectively. *C*, IL-12p40 prefers the heterodimeric p70 form over homodimeric interactions. Shown is a comparison of extracellular samples from cells transfected with p40 alone (300 ng; *lane 1*) and p40 + p35 (300 ng of p40 plus 100 ng of p35; *lane 2*) under native (without β-mercaptoethanol, without SDS; *top*), non-reducing (without β-mercaptoethanol, plus SDS; *middle*), and reducing (treated with β-mercaptoethanol and with SDS; *bottom*) conditions. *D*, stability of human p35 and p40 subunits upon treatment with CHX. At 1 day posttransfection, the medium was replaced with fresh medium containing CHX (see "Experimental Procedures"). The cell-associated and extracellular fractions were collected at 0, 1, 2, and 4 h and analyzed on Western immunoblots. The bands were quantitated, and the accumulation of p35 and p40 when transfected alone or in combination was calculated over time by normalizing the value (sum of extracellular and cell-associated) at the start of the CHX treatment (time 0) as 100%. p35 (*open circles*), p40 alone (*open squares*), and a mixture of the p35 and p40 subunits (*filled triangles*) are shown. A combination of 2–3 independent experiments is shown.

respective subunits, the level of the secreted p35 was significantly enhanced (*lane 3*) as shown above (Fig. 1*A*), resulting in the production of the IL-12p70 heterodimer as confirmed by the IL-12p70-specific ELISA (*bottom panel*). Together, we found that the total amount of the p35 subunit was greatly increased by the presence of p40 (Fig. 1*B*, compare *lanes 1* and

*3*), supporting the conclusion that p40 has a positive effect on the steady-state level of p35.

To determine the optimal levels of each subunit for the production of IL-12p70, we cotransfected different ratios of p35/p40 plasmids, namely 1:1 (Fig. 1*B*, *lane 3*), 1:3 (*lane 4*), and 3:1 (*lane 5*). We noted that a higher amount of the p40 plasmid (p35/p40 plasmid ratio 1:3; *lane 4*) led to further augmentation of the extracellular levels of IL-12p70 heterodimer, indicating that the p40 levels were limiting upon cotransfection of a 1:1 ratio of the p35 and p40 plasmids. These data were confirmed by the IL-12p70-specific ELISA (Fig. 1*B*, *bottom*). Cotransfection of more p40 plasmid (ratio 1:8) did not show substantial improvement (data not shown). In contrast, increasing the amount of the p35 plasmid (p35/p40 plasmid ratio 3:1; *lane 5*) led to slightly lower IL-12p70 production, with appreciable amounts of the p35 subunit trapped in the intracellular compartment (Fig. 1*B*, *lane 6*, *top*). These data support the conclusion that the p40 subunit drives the production and secretion of stable heterodimeric IL-12p70 (Fig. 1*B*, *lanes 3* and *4*).

The p40 homodimer was reported to bind with IL-12 receptor but lacks any IL-12 bioactivity (16, 38), and it was reported to interfere with IL-12p70 function (17, 40, 41). Because we co-expressed excess p40 by providing more p40 DNA to obtain optimal IL-12p70 production, we investigated whether free p40 homodimer accumulated under this condition. We compared the status of the extracellular p40-FLAG when present alone (Fig. 1*C*, *lane 1*) and in the presence of p35 (*lane 2*) under native, non-reducing, and reducing conditions. Analysis under reducing conditions confirmed the presence of similar amounts of p40 in both samples (Fig. 1*C*, *bottom*). Analysis of p40 under native conditions showed the presence of both monomer and homodimer (16, 17), with the majority of the protein in the homodimeric form (Fig. 1*C*, *top*, *lane 1*). In the presence of p35, a significant reduction in both forms of p40 was found with a concomitant association of p40 with p35, forming the heterodimeric p70 (Fig. 1*C*, *top*, *lane 2*). To further distinguish between the homodimeric and heterodimeric forms of p40, we analyzed these samples under non-reducing conditions (upon treatment with SDS; Fig. 1*C*, *middle*). This showed that the p40 homodimers disappeared in the presence of p35 (compare *lane 1* and *lane 2*), indicating preferential formation of the p70 heterodimer. Even under this extreme condition of p40 excess production, only trace amounts of p40 homodimer were found, and they are unlikely to significantly interfere with IL-12p70 function (40), which is produced in large excess. These data suggest that, because p40 is efficiently exported, increased intracellular levels are necessary to allow interaction with the unstable p35 to occur. Thus, a fine balance of the two subunits is critical for optimal production of the cytokine.

*The IL-12p40 Subunit Stabilizes the IL-12p35 Subunit*—To understand the mechanisms leading to increased levels of p35 in the presence of p40, we performed pulse-chase experiments with CHX. We compared the stability of the human IL-12p35 and p40 subunits when expressed alone or together (Fig. 1*D*). Transfected HEK293 cells were treated with CHX and monitored for up to 4 h. The cell-associated fractions and supernatants were analyzed by Western immunoblot assays, and the bands were quantified and presented as total p35 or p40. This

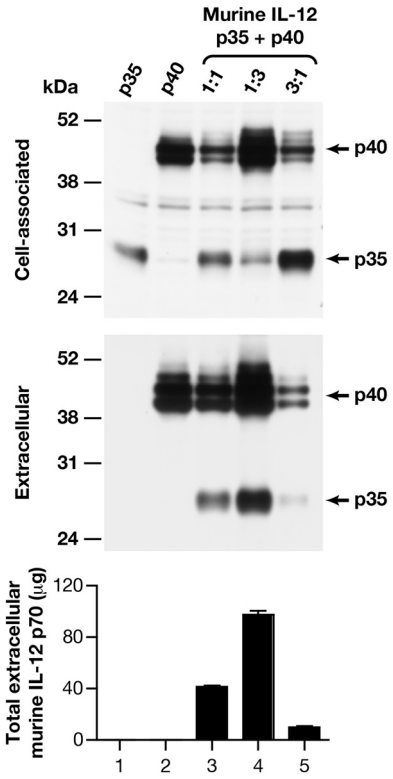


FIGURE 2. **Role of p40 is conserved for the murine IL-12p70 production.** Optimization of co-expression of the murine IL-12 subunits expressed alone (*lanes 1* and *2*, respectively) or together using the indicated plasmid ratios is shown. Cell-associated (*top*) and extracellular (*middle*) fractions were analyzed by a Western immunoblot assay and by a murine IL-12p70-specific ELISA (*bottom*). The mean of two independent plasmid preparations and the S.E. (*error bars*) are shown. The GFP values (mean ± S.E.) were 10.6 ± 0.4, 23.3 ± 1.2, 16.2 ± 0.1, 19.0 ± 0.1, and 8.1 ± 0.1 arbitrary units for *lanes 1–5*, respectively.

analysis demonstrated that the p35 subunit has a half-life of ~2 h, when expressed alone. This finding is in agreement with a previous report (39) that suggested a relative short half-life of ~3 h. Importantly, we found that the stability of p35 was greatly increased to >4 h in the presence of p40 (*top panel*). In contrast, the p40 subunit half-life was >4 h, and as expected, it was not affected by the presence of p35 (*bottom panel*). These data demonstrate that the interaction of IL-12p40 with p35 led to its stabilization, which supports the observed increased steady-state level of the p35 subunit. Consequently, the interaction of the two molecules also affected the trafficking of the p35 subunit (Fig. 1, *A* and *B*), resulting in increased secretion of the mature IL-12p70 heterodimer (Fig. 1*B*, *bottom*). We noted an overall increase in the stable forms (*i.e.* of p40 alone or in the presence of p35 and of p35 in the presence of p40), reflecting the extracellular accumulation of the subunits produced prior to the CHX addition.

*The Regulation of IL-12p70 Production by Its p40 Subunit Is a Conserved Regulatory Mechanism*—We also tested the production of the murine IL-12p70 heterodimer from RNA/codon-optimized coding sequences (Fig. 2) upon transfection in HEK293 cells using the same methods as described for Fig. 1*B*. The murine p35 subunit expressed alone remained cell-associated (Fig. 2, *lane 1*), whereas the murine p40 subunit was found both in the intra- and extracellular compartments (*lane 2*).

Cotransfection of both subunits resulted in efficient export of the p35 subunit (*lane 3*), similar to their human counterparts. Production of the heterodimeric IL-12 was confirmed using the murine IL-12p70-specific ELISA (Fig. 2, *bottom*). Like for human IL-12 (Fig. 1, *A* and *B*), we found increased steady-state levels of the p35 subunit upon co-expression with p40 (Fig. 2, compare *lanes 1* and *3*). Cotransfection of higher amounts of the murine p40 plasmid (p35/p40 plasmid ratio 1:3; *lane 4*) further augmented both the p35 steady-state level and export, leading to the production of higher levels of murine IL-12p70. In contrast, excess of the p35 plasmid (*lane 5*) decreased the extracellular p40 and the IL-12p70 levels. Similar data were obtained upon transfection of the NIH3T3-derived murine PA317 cells (data not shown), indicating that this is a general property of the IL-12 subunits independent of the species of the producer cells. Thus, the studies of the human and murine subunits revealed a critical role of p40 in mediating stabilization and promoting trafficking and secretion of p35, suggesting that this is a conserved regulatory step in the biosynthesis of IL-12p70 heterodimer in mammals.

*Co-expression of the Human p35 and p40 Subunits Alters Their Subcellular Localization*—To study the effect of p40 on p35, the intracellular localization of p35 was investigated. Cells transfected with plasmids expressing the FLAG-tagged subunits, alone or in combination, were examined by fluorescent microscopy (Fig. 3*A*). The p35-FLAG (Fig. 3*A*) was found in punctate foci in the cytoplasm when expressed alone. Several cellular markers with known localization, such as calreticulin for the ER, Rab5 for early endosomes, and Rab11 and transferrin for recycling endosomes, were tested, but no colocalization with p35-FLAG was found, indicating that p35 did not accumulate appreciably in the ER. The p40-FLAG was also found in punctate foci in the cytoplasm (Fig. 3*E*) and did not colocalize with the above listed markers, also indicating no appreciable accumulation in the ER. When present alone, a minority of the p35-FLAG (~10%) and p40-FLAG (~14%) colocalized with TGN46, a marker for the trans-Golgi network (TGN), a system of membranes responsible for the sorting of proteins. Cotransfection of plasmids expressing the FLAG-tagged subunit with its untagged partner led to a significant change in the localization of the p35 and p40 subunits to the perinuclear area (Fig. 3, *I* and *M*, respectively), compatible with Golgi localization. Staining of the cells with TGN46 demonstrated that the FLAG-tagged p35 (~91% of cells; Fig. 3*L*) and p40 (~89% of cells; Fig. 3*P*), respectively, significantly co-localized with TGN46, indicating more efficient association with the trans-Golgi network when expressed together. Accumulation at the Golgi is only found in the presence of the two partners and is critical for the export of the heterodimer, supporting the notion that this colocalization reflects a transient accumulation in the Golgi. Together, these data demonstrate that p40 increased the stability of p35 (Fig. 1*D*) and promoted the intracellular trafficking of the p35 subunit through the Golgi export pathway (Fig. 2*A*).

*The IL-12p40 Chain Enhances the Mobilization of IL-12p35 to the Golgi*—Because p40 promoted the TGN association of p35, we asked whether coexpression with p40 affects the post-translational modification of p35. Glycosylation of the p35 subunit has been shown to be essential for the assembly and secretion of the cytokine, whereas the p40 subunit is secreted irrespective of its glycosylation status (38, 39). We investigated the sensitivity of the coexpressed human IL-12 subunits to digestion with endoglycosidases. Extracts from transfected cells were treated *in vitro* with Endo H and Endo F, two endoglycosidases used to interrogate protein glycosylation during export and to monitor posttranslational modifications taking place in the ER and Golgi. Endo H cleaves asparagine-linked mannose-rich oligosaccharides but cannot cleave the complex modified sugars acquired during protein trafficking through the Golgi, whereas Endo F can cleave both simple and complex sugars and acts as positive control to evaluate the presence of *N*-linked sugar moieties. The individual p35 (39, 42) and p40 (39) subunits, when present alone, have been reported to have distinct sensitivity to these endoglycosidases; the intracellular p35 was sensitive to cleavage by Endo H and Endo F (Fig. 3*B*, *lanes 1–3*), whereas the extracellular p35 was Endo H-resistant but Endo F-sensitive, indicating that p35 acquired complex glycosylation while being exported via the Golgi (*lanes 1–3*, *right*). Because its levels were very low in the absence of p40, we were unable to detect an Endo H-resistant form. The p40 subunit did not undergo complex glycosylation, and both the cell-associated and extracellular forms could be digested with both enzymes (Fig. 3*B*, *lanes 4–6*, *left* and *right*), indicative of a lack of modification with complex oligosaccharides. Previous works reported only on the subunits when present alone (38, 39); however, because our work focuses on understanding the effect of p40 on p35 biosynthesis, we subjected extracts containing both subunits to Endo H and Endo F treatment. Interestingly, when coexpressed with p40, we noted the appearance of a minor higher molecular mass ~36 kDa band of p35 in the cell-associated fraction (Fig. 3*B*, *lane 7*, *left*), which was Endo H-resistant (*lane 8*, *left*). This band comigrated with the extracellular Endo H-resistant p35 (Fig. 3*B*, *lane 8*, *right*) and probably represents p35 in the process of trafficking, which has acquired complex sugars while traveling through the Golgi. Because this is a transient stage, p35 is not expected to accumulate intracellularly as an Endo H-resistant form, and indeed our studies showed that p35 was efficiently exported in the presence of p40 and did not accumulate in the cell-associated fraction. Although in the absence of p40, the p35 subunit undergoes similar modifications (see the presence of Endo H-resistant p35 in the supernatant; Fig. 3*B*, *lane 2*, *right*), its overall steady-state levels were very low because p35 by itself is unstable and poorly secreted, and thus, this intermediate form could not be detected in the cell-associated fraction (Fig. 3*B*, *lane 2*, *left*). Taken together, our data revealed critical steps for the synthesis of bioactive IL-12p70 controlled by the p40 subunit, which mobilized p35 and promoted its trafficking to the Golgi, where the sugars on p35 were subjected to complex modification prior to the secretion of the mature heterodimeric IL-12p70.

*Generation of Optimized IL-12 Dual Promoter Plasmids for in Vivo Gene Delivery*—IL-12 DNA-based *in vivo* applications require coordinated optimal expression of both IL-12 subunits within a cell, which can be better achieved with a single plasmid producing both p35 and p40 subunits. Two dual promoter vectors with slightly different plasmid backbones (vector pWLV-009M (31) and pDP (43)) were compared for the production of

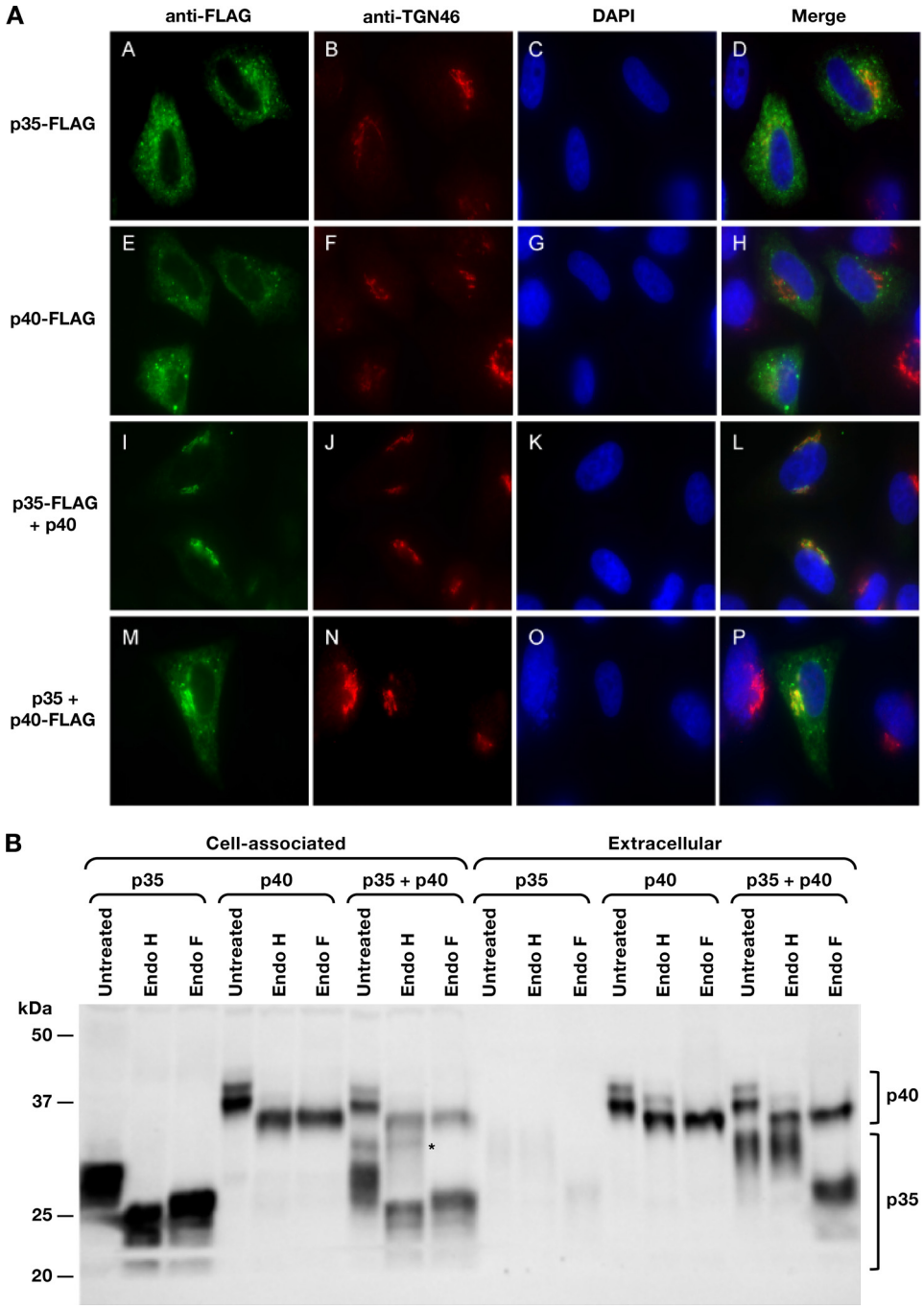


FIGURE 3. **The coexpression of human IL-12p35 and p40 alters intracellular localization.** *A*, HLtat cells were transfected with p35-FLAG (*A–D*), p40-FLAG (*E–H*), and the combinations of p35-FLAG and p40 (*I–L*) or p35 and p40-FLAG (*M–P*) and fixed. FLAG-p35 and FLAG-p40 were visualized with anti-FLAG primary followed by Alexa-Fluor 488 secondary antibody (*A*, *E*, *I*, and *M*). The TGN was visualized with anti-TGN46 primary antibody followed by Alexa-Fluor 594 secondary antibody (*B*, *F*, *J*, and *N*). The nuclei were visualized with DAPI (*C*, *G*, *K*, and *O*). The images were merged to show similar localization within the TGN (*D*, *H*, *L*, and *P*). *B*, increase of glycosylated p35 in the presence of p40. The supernatants and cell lysates from HEK293 cells transfected with plasmids expressing the individual p35 or p40 subunits either alone or together were treated with Endo F or Endo H or left untreated. The samples were analyzed by Western immunoblot assay using the human IL-12p70 antibody. *, Endo H-resistant forms of p35 in the cell-associated fraction.

IL-12p70. Both vectors contain the strong huCMV and the weaker siCMV promoters, controlling the expression of the IL-12 subunits in counterclockwise orientation. The human, rhesus macaque, and murine IL-12 subunits were cloned into these vectors, taking into consideration the contribution of the RNA-optimized gene sequences and the importance of the relative ratio (see Fig. 1) of the subunits for optimal IL-12p70 production. Expression of the plasmids was compared upon transient transfection in HEK293 cells and analyzed by Western immunoblot and ELISA assays (Fig. 4).

For the human IL-12p70 (Fig. 4*A*), the use of RNA-optimized p35 and p40 coding sequences led to a ~2-fold increase in IL-12p70 production (Fig. 4*A*, *lane 2*, plasmid AG5) when compared with the plasmid expressing the native sequences (*lane 1*,

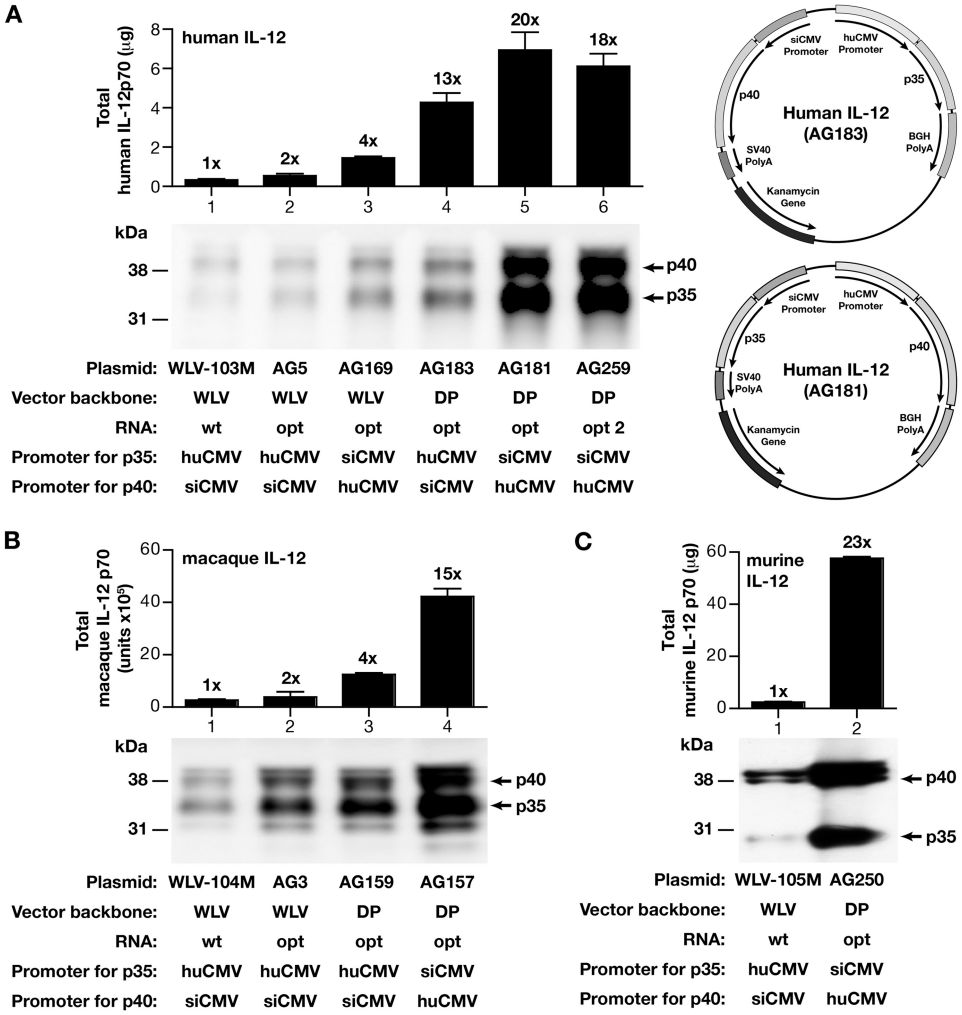


FIGURE 4. **Optimized dual promoter expression vectors for improved IL-12p70 production.** *A*, expression of the human IL-12p70 from different dual promoter plasmids. IL-12 production was measured by human IL-12p70-specific ELISA (*top*) and by a Western immunoblot assay (*bottom*). The plasmids contain the following: wild type human IL-12 coding sequences expressed from WLV-009M (plasmid WLV-103M; *lane 1*) and RNA-optimized coding sequences expressed from vectors WLV-009M (plasmid AG5 (*lane 2*); plasmid AG169 (*lane 3*) and pDP (plasmid AG183 (*lane 4*); plasmid AG181 (*lane 5*); plasmid AG259 (*lane 6*)). The two configurations of dual promoter (*DP*) human IL-12 plasmids expressing the p35 and p40 coding sequences from the huCMV or the siCMV promoters are shown on the *right*. The GFP values (mean ± S.E. (*error bars*)) for *lanes 1–6* were 17.3 ± 5.7, 22.1 ± 2.3, 20.0 ± 1.6, 25.4 ± 3.3, 27.3 ± 4.0, and 25.6 ± 1.2 arbitrary units, respectively. *B*, expression of the rhesus macaque IL-12p70 from different dual promoter plasmids. The IL-12 production was measured by a macaque IL-12p70-specific ELISA (*top*) and by a Western immunoblot assay (*bottom*) from transfected cells. The plasmids contain the following: wild type macaque coding sequences expressed from the dual promoter plasmid WLV-009M (plasmid WLV-104M; *lane 1*) and RNA-optimized coding sequences expressed from vectors WLV-009M (plasmid AG3; *lane 2*) and pDP (plasmid AG159 (*lane 3*) and plasmid AG157 (*lane 4*), respectively). The GFP values (mean ± S.E.) for *lanes 1–4* were 19.7 ± 1.0, 20.5 ± 1.3, 11.9 ± 1.6, and 16.2 ± 0.9 arbitrary units, respectively. *C*, expression of an optimized murine IL-12p70 plasmid. The IL-12 production was measured using a murine IL-12p70-specific ELISA (*top*) and by the Western immunoblot assay (*bottom*). The plasmids contain the following: wild type murine coding sequences expressed from the dual promoter plasmid WLV-009M (plasmid WLV-105M; *lane 1*) and RNA-optimized coding sequences expressed from vector pDP (plasmid AG250; *lane 3*). The GFP values (mean ± S.E.) for *lanes 1* and *2* were 8.4 ± 0.8 and 11.6 ± 0.6 arbitrary units, respectively.

plasmid WLV-103M (31, 44, 45)). To obtain favorable relative levels of the p35 and p40 subunits, the p40 subunit was placed under the control of the stronger huCMV promoter (Fig. 4*A*, *lane 3*, plasmid AG169), which led to a further 2-fold increase (compare *lanes 2* and *3*) and an overall 4-fold increase in IL-12p70 production (compare *lanes 1* and *3*). These data underscore the observation that the p40 level is driving the efficient IL-12p70 heterodimer production and that the selection of promoters in the dual promoter plasmid can mimic our observation from the transfection using single promoter plasmids.

A further improvement (~5–6-fold) of IL-12 expression was obtained upon substitution of the vector pWLV-009M with the vector pDP (Fig. 4*A*, compare *lanes 2* and *4* or *lanes 3* and *5*, respectively). The pDP vector consistently yielded higher levels of IL-12p70 expression. Comparison of the configurations (huCMV-p35/siCMV-p40 as in plasmid AG183 or huCMV-p40/siCMV-p35 as in plasmid AG181; see Fig. 3*A*, *right panels*) confirmed that expression of the p40 subunit from the huCMV promoter resulted in higher IL-12 production (Fig. 4*A*, compare *lanes 4* and *5*). Testing of another IL-12p70 plasmid (AG259; *lane 6*), which encodes variants of RNA/codon-optimized p35 and p40 coding sequences showed no significant differences in expression levels (compare *lanes 6* and *5*), indicating that maximal IL-12p70 production was achieved (plasmid AG181, *lane 5*). Together, the different optimization steps,

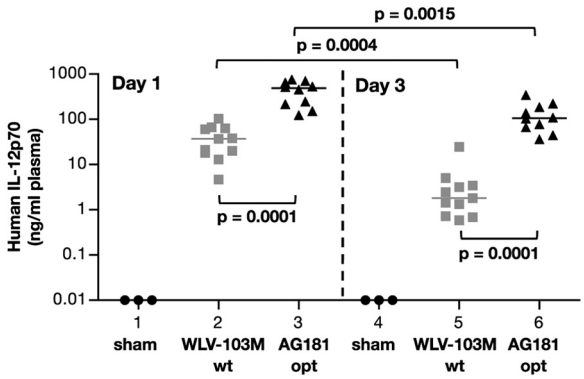


FIGURE 5. ***In vivo* expression of IL-12p70 plasmids in mice.** Expression of the human IL-12p70 DNA was tested in BALB/c mice upon hydrodynamic DNA delivery. The animals ($n = 10–11$/group) were injected with 100 ng of a plasmid expressing the IL-12 from wild type (WLV-103M; *lanes 2* and *5*) or from optimized coding sequences (plasmid AG181; *lanes 3* and *6*). The sham control group ($n = 3$) was injected with 100 ng of the empty vector pCMVkan (*lanes 1* and *4*). The mice were bled at day 1 (*lanes 1–3*) and sacrificed at day 3 (*lanes 4–6*) postinjection. Plasma samples were analyzed by a human IL-12p70-specific ELISA, and the values of individual mice and median are shown. *p* values using the Mann-Whitney *t* test are shown.

including coding sequence RNA optimization, vector, and promoter selection resulted in ~20-fold improvement of human IL-12p70 production.

Using a similar strategy, we generated optimized dual expression plasmids for rhesus macaque IL-12p70 (Fig. 4*B*). Consistent with the findings of the human IL-12p70, the use of RNA-optimized coding sequences, expression of the p40 subunit from the stronger human CMV promoter, and the selection of the expression plasmid (pDP) led to the greatest increase in rhesus macaque (~15-fold; Fig. 4*B*, *lane 4*) IL-12p70 production.

We also generated an optimized dual promoter expression plasmid for the murine IL-12p70, taking into consideration the expression vectors (see above), the contribution of the RNA-optimized gene sequences, and the importance of the relative ratio (see Fig. 1*D*) of the subunits for optimal cytokine production. Supernatants from HEK293 transfected cells were analyzed by Western immune blot assay and p70-specific ELISA (Fig. 4*C*). These data showed that optimization of expression (plasmid AG250) led to ~20-fold increase compared with IL-12 produced from a vector expressing the wild type genes from suboptimal vector in suboptimal configuration (compare *lanes 1* and *2*). Together, the combination of RNA/codon-optimized coding sequences, the choice of the dual promoter expression vector, and the configuration of the subunits within the dual promoter plasmid showed a net increase of ~1 log for human, macaque, and murine IL-12p70 production.

*In Vivo Expression of Human IL-12p70 DNA in Mice*—We further evaluated the *in vivo* production of human IL-12p70 from different plasmids upon hydrodynamic DNA delivery into BALB/c mice (Fig. 5). The animals received 100 ng of plasmids expressing the IL-12p70 from wild type sequences (*Plasmid WLV-103M*, *wt*) and from RNA-optimized coding sequences (*Plasmid AG181*, *opt*) or sham DNA, respectively. At days 1 and 3 postinjection, the levels of the IL-12p70 heterodimer were measured in plasma using the human IL-12p70-specific ELISA (Fig. 4). Sham DNA-injected mice (*lanes 1* and *4*) did not show any detectable human IL-12 (threshold of the assay 0.015 ng/ml). At day 1, the mice receiving the wild type plasmid had a median IL-12p70 plasma level of 37 ng/ml (*lane 2*), whereas the mice receiving the optimized plasmid (*lane 3*) had a median of 489 ng/ml. These data show a significant ~13-fold higher IL-12p70 production from the optimized human IL-12 plasmid and are in agreement with the observed difference between the plasmids upon transient transfection (Fig. 4*A*). This difference also remained significant at day 3 (*lanes 5* and *6*), with 1.8 and 107 ng/ml IL-12p70 for the mice that received the wild type and the optimized plasmids, respectively. Interestingly, we also noted a significantly slower apparent decay ($p = 0.0004$) of IL-12 in the plasma levels produced from optimized plasmid (~4-fold decline, $p = 0.0015$; *lanes 3* and *6*) compared with the wild type plasmid (~20-fold decline, $p = 0.0004$; *lanes 2* and *5*), suggesting that the optimized RNA is more stable *in vivo*, resulting in longer IL-12p70 expression. Because the human IL-12 is not active in mice, bioactivity could be tested in this experiment.

*Bioactivity of IL-12 upon in Vivo Delivery of Optimized Murine IL-12p70 DNA in Mice*—Next, we compared expression of murine IL-12p70 plasmids in BALB/c mice (Fig. 6). The plasmids consisting of the wild type (*WLV-105M*, *wt*) and the RNA-optimized (*AG250*, *opt*) murine IL-12p70, described in Fig. 2, or sham DNA were delivered by intramuscular injection followed by *in vivo* electroporation (5 $\mu$g of DNA/mouse; $n = 5$/group). Plasma samples were collected at days 3 and 6 post-DNA injection, and cytokine production was measured by a murine IL-12p70-specific ELISA (Fig. 6*A*). Sham DNA-injected mice (*lanes 1* and *4*) did not show detectable IL-12p70 levels (threshold of the assay, 0.015 ng/ml). The optimized plasmid produced significantly higher IL-12p70 levels with a median of 4 ng/ml plasma (*lane 3*) compared with 0.46 ng/ml (*lane 2*) from the wild type plasmid at day 3 postinjection. Thus, the production from the optimized plasmid in mice is ~10-fold higher, and we found a similar difference upon transient transfection of these plasmids in human HEK293 cells. This ~1 log difference in IL-12 levels also remained significant at day 6, with IL-12p70 levels of 0.09 ng/ml obtained from the wild type plasmid and 1.07 ng/ml from the optimized plasmid, respectively.

The plasmids led to production of systemically active IL-12p70 in mice, which led to induction of IFN-$\gamma$ production (Fig. 6*B*). Sham DNA-injected BALB/c mice (*lanes 1* and *4*) did not show detectable IFN-$\gamma$ levels (threshold of the assay, 0.0007 ng/ml) indicating that the IFN-$\gamma$ produced was due to IL-12 and not an effect of *in vivo* electroporation. Animals receiving the optimized plasmid produced significantly higher levels of IFN-$\gamma$ in the plasma (*bottom panel*) with a median of 0.8 ng/ml (*lane 3*) as compared with wild type plasmid (0.37 ng/ml; *lane 2*) at day 3. The significant difference in IFN-$\gamma$ levels also remained at day 6, when median levels of 0.06 and 0.26 ng/ml of plasma IFN-$\gamma$ were measured. There was a direct correlation between the levels of IL-12p70 and IFN-$\gamma$ ($r = 0.8872$, $p < 0.0001$; Fig. 5*C*), demonstrating the biological activity of plasmid-produced IL-12p70.

*Optimized IL-12 DNA Provides More Potent Control of B16 Melanoma Growth in Mice*—To examine the biological activity of our DNA plasmids, we also compared the anti-tumoral

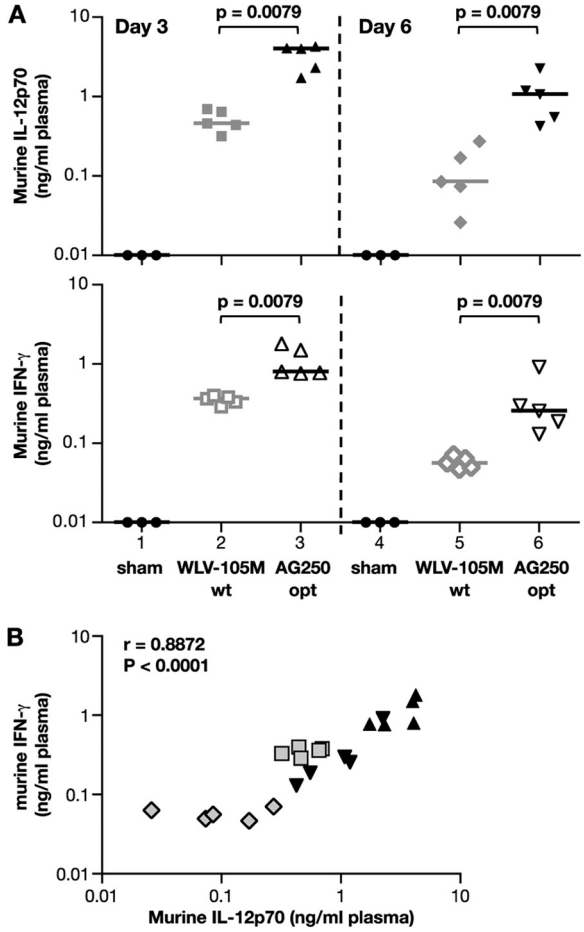


FIGURE 6. ***In vivo* expression and bioactivity of murine IL-12 plasmids.** *A*, production of bioactive murine IL-12p70 *in vivo*. Plasmids (5 $\mu$g/animal) expressing the murine IL-12p70 were injected intramuscularly, followed by *in vivo* electroporation into BALB/c mice ($n = 5$/group). The dual gene expression plasmids contain the following: wild type coding sequences (WLV-105M; *lanes 2* and *5*) or optimized coding sequences (plasmid AG250; *lanes 3* and *6*). The sham control group ($n = 3$) was injected with 100 $\mu$g of the empty vector (CMVkan; *lanes 1* and *4*). The mice were bled at day 3 and sacrificed at day 6 postinjection. Individual mouse plasma samples were analyzed for the levels of murine IL-12p70 (*top*) and murine IFN-$\gamma$ (*bottom*) by the respective ELISA. The values from the individual mice and median values are shown. *p* values using Mann-Whitney two-tailed *t* test are shown. *B*, *r* and *p* values using Spearman nonparametric correlation between the murine IL-12p70 levels and the murine IFN-$\gamma$ levels from the mice, depicted in Fig. 5*A*.

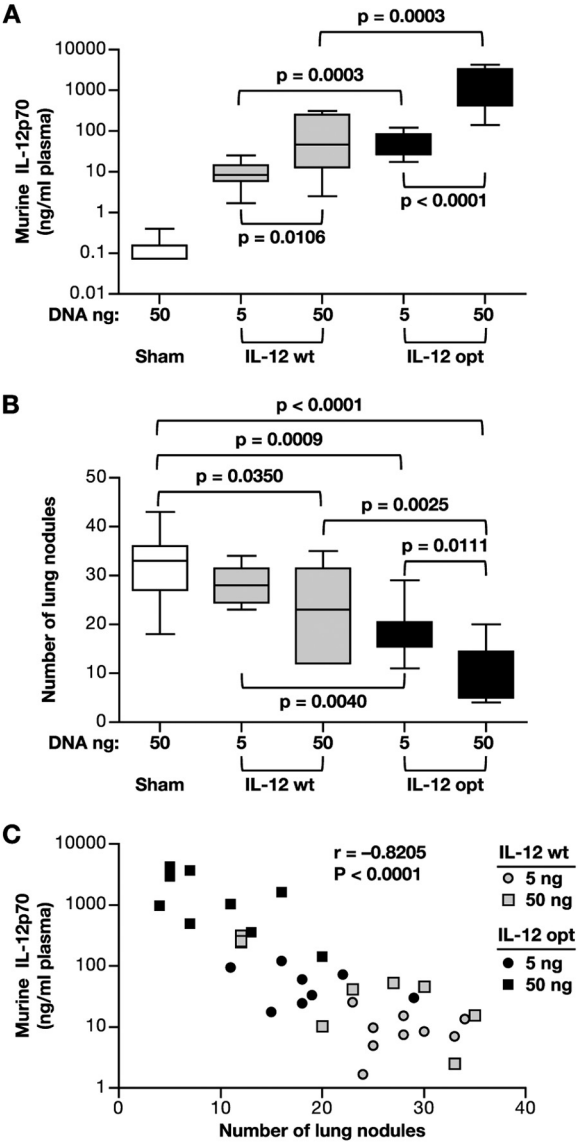


FIGURE 7. **Murine IL-12 DNA treatment of B16 melanoma tumor.** *A*, C57BL/6 mice (groups of 9–10 mice) were inoculated with $10^5$ B16 melanoma cells via the intravenous route. Two days later, 5 or 50 ng of the wild type (plasmid WLV-105M) or optimized (plasmid AG250) murine IL-12 DNA were injected using hydrodynamic DNA delivery. Sham vector DNA (CMVkan; 50 ng) was injected into the control mice. Mice were bled at day 1 post-DNA injection, and the plasma levels of murine IL-12p70 were determined. *B*, after 3 weeks, the mice were sacrificed, and the lung nodules were counted (*bottom*). *p* values using the Mann-Whitney two-tailed *t* test are shown. *C*, correlation of plasma IL-12 levels (measured at day 1 post-DNA injection) and number of lung nodules (at week 3 post-tumor injection) from the data shown in Fig. 6*A*. *Error bars*, S.E.

effects of the low and high murine IL-12p70-expressing plasmids in a B16 melanoma cancer model. C57BL/6 mice were inoculated with B16 melanoma cells, and 2 days later the animals received a single administration of IL-12 DNAs expressing low (plasmids WLV-105M, wild type) or high (plasmid AG250, optimized) levels of murine IL-12p70 or control DNA via hydrodynamic delivery. Two doses of each DNA (5 and 50 ng, respectively) were tested. The IL-12p70 plasma levels were determined at 1 day after DNA injection (Fig. 7*A*), and after 3 weeks, the mice were sacrificed and tumor nodules in lungs were counted (Fig. 7*B*).

Sham DNA-injected mice C57BL/6 mice showed very low IL-12p70 levels (Fig. 7*A*) with a median of 0.075 ng/ml (threshold of the assay, 0.015 ng/ml). Injection of wild type IL-12 plasmid yielded median IL-12p70 levels of 8.5 and 47 ng/ml plasma, respectively, whereas the optimized plasmid yielded median levels of 47 and 1,051 ng/ml plasma, respectively. Injection of the higher amount of DNA resulted in significantly higher IL-12p70 levels for both of the plasmids ($p = 0.0106$ for wild type DNA and $p < 0.0001$ for optimized plasmid). At both concentrations, the optimized plasmid produced significantly higher levels of IL-12 ($p = 0.003$ for 5 and 50 ng of IL-12 plasmid, respectively). These data reflect a difference in IL-12p70 production from these plasmids similar to that obtained upon transient transfection (Fig. 2) and intramuscular delivery in mice (Fig. 6*A*) and show that the 50-ng DNA dose of the wild type plasmid is giving IL-12p70 levels similar to those given by the 5-ng dose of the optimized plasmid.

Enumeration of the lung tumors after 3 weeks revealed a significant reduction in the number of nodules in mice that received the IL-12 DNA (50 ng of wild type plasmid, $p = 0.0350$; 5 ng of optimized plasmid, $p = 0.0009$; 50 ng of optimized plasmid, $p < 0.0001$), except for the animals that received the low dose of the wild type plasmid (Fig. 7*B*). The extent of tumor growth control reflected the IL-12p70 plasma levels in each of the treated groups. We noted significant reductions in tumor burden, comparing the low ($p = 0.0040$) and high dose ($p = 0.0111$) of the wild type and the optimized plasmids, respectively, with 50 ng of the high IL-12 producer (plasmid AG250) being the most potent (*bottom panel*; $p < 0.0001$). Consequently, there was a significant ($r = -0.8205$, $p < 0.0001$) inverse correlation between the IL-12p70 plasma levels and the number of tumor nodules, indicating that high levels of systemic IL-12p70 were crucial for preventing the establishment of lung metastasis in this model (Fig. 7*C*). Thus, the use of the high level expression plasmid increased the potency of the IL-12p70 DNA for *in vivo* applications.

## DISCUSSION

The IL-12 family of heterodimeric cytokines (IL-12, IL-23, IL-27, and IL-35) uses intracellular molecular interactions between the different subunits to regulate the production of the bioactive cytokines (3, 4, 46, 47). It is thus essential to understand the molecular basis of this regulation involving multiple steps at the transcriptional, posttranscriptional, and posttranslational level for the rational design of expression vectors that can be translated into clinical applications. In the present study, we have identified a novel role of IL-12p40 for the stabilization and trafficking of the IL-12p35 subunit. This role is shared by the human, macaque, and murine p40 subunits, suggesting a conserved mechanism of IL-12 regulation in different mammals. It was previously shown that the two IL-12 subunits interact in the ER (38, 39). Herein, we demonstrate that the level of p40 is key for productive interaction with p35 and for optimal biosynthesis of IL-12p70 heterodimer. In fact, its absence is the rate-limiting factor for the efficient export of the p35 subunit through the Golgi, where complex glycosylation takes place, providing the modifications essential for the secretion of mature heterodimeric IL-12p70 (38). We found that a fine balance between the two subunits, with higher levels of p40, is necessary for efficient IL-12p70 production. It was previously reported that low levels of p35 (48, 49) or the efficiency of its glycosylation (38) were the limiting factors for the production of IL-12. In contrast, our work shows that the relative amount of the two subunits is the decisive factor determining the efficiency of IL-12 production; a fully functional p40 present at excess is critical for directing the transport of p35, maximizing the secretion of p70 heterodimer. The novel role of p40 in enhancing the posttranslational stability and trafficking of p35 described herein provides the molecular rationale for p40 to be expressed as stable protein at high levels. Previous studies reported that cells that secrete bioactive IL-12p70 also secrete p40 in free form in excess over the IL-12 heterodimer (2, 50, 51), demonstrating constitutively higher levels of p40 expression, which, according to our data, is critical for the IL-12p70 production. We find very little, if any, extracellular p40 homodimer when the two subunits are expressed optimally in the same cell. Our model explaining all data suggests that formation of p40 homodimers is slow and inefficient, whereas the p40-p35 heterodimers are formed rapidly at a rate dictated by the availability of p40. Therefore, the presence of p35 in the same cell results in only the heterodimer being effectively produced.

The observation about the concerted export of the p35 subunit by p40 is reminiscent of the production of IL-15, which is another heterodimeric cytokine (18–21) (for a review, see Ref. 52). IL-15 consists of two chains, the IL-15 and the IL-15R$\alpha$, which together form the circulating form found in plasma (20). We and others (18, 19, 53–55) previously reported that co-expression of IL-15 and IL-15R$\alpha$ within the same cell leads to rapid intracellular association of the chains in the ER, resulting in the stabilization of both molecules and the translocation of the complex through the Golgi to the cell membrane, where it is bioactive and from where it is rapidly cleaved and released as a functional extracellular cytokine (18, 19). The steps of the biosynthesis of IL-15 and IL-12 share numerous similarities, as follows: (i) one of the heterodimeric components (IL-12p35, IL-15) is unstable and exists in different isoforms distinguished by the size of the signal peptides (18, 39, 42, 56, 57); (ii) IL-12p35 and IL-15 are secreted very poorly when expressed alone; (iii) they form a stable complex with their respective partner in the ER (IL-12p35 and IL-12p40 are linked via a disulfide bridge; IL-15 and IL-15R$\alpha$ form a high affinity complex); and (iv) IL-12p40 and IL-15R$\alpha$ stabilize their respective partner molecules and promote their trafficking through the Golgi and export of the complex. Thus, IL-12 and IL-15 are two heterodimeric cytokines, which undergo similar steps of posttranscriptional and posttranslational regulation.

Optimized IL-12-expressing vectors are desirable for many potential clinical applications in cancer therapy (58–65) (reviewed in Refs. 6, 7, 63, and 66) as well as molecular adjuvants for vaccines (22, 31, 43–45, 67). Expression of both subunits within a cell can be achieved by generating an artificial single chain molecule (68, 69) or by a single plasmid expressing both of the subunits from two independent promoters. We pursued the latter approach, based on the knowledge we gained examining the molecular interactions between the two IL-12 subunits. This led us generate optimized DNA expression vectors with the optimal configuration for the production of both p35 and p40 and efficient IL-12p70 secretion. In this report, we also showed a significant contribution not only from optimizing the gene sequences and the relative expression levels but importantly also the selection of expression vector. The combined optimization strategies resulted in >1 log increase in human, rhesus, and murine IL-12p70 expression compared with vectors expressing the wild type sequences. These optimized vectors were used *in vivo* in two different animal models. Comparisons show that the improvements found in HEK293 cells were reproduced also in mice. Similar results were obtained upon systemic delivery by hydrodynamic DNA injection as well as local muscle DNA injection (Figs. 5–7). Thus, we tested the basic concept of improvement of expression in different species and tissues with comparable conclusions. In addition, we showed that intramuscular injection of the optimized rhesus IL-12 expression plasmid (AG157), followed by *in vivo* electro-

poration, resulted in detectable IL-12p70 plasma levels in rhesus macaques (43). The elevated levels of IL-12 were paralleled by a rapid increase of plasma IFN-γ, reflecting the bioactivity of the IL-12 encoded by the vector. Furthermore, in a proof-of-principle study described in this paper using a melanoma mouse lung tumor model, we showed that treatment with the optimized murine IL-12 DNA is more potent than treatment with the plasmid expressing the wild type coding sequences in controlling tumor growth (Fig. 6). Thus, in mice and macaques, the use of high expression IL-12 plasmids resulted in the production of systemic IL-12p70 and IFN-γ levels. We have extended the use of optimized macaque IL-12p70 vectors to other *in vivo* applications. IL-12 DNA was delivered into rhesus macaques together with a SIVmac239 DNA vaccine as a molecular adjuvant (43, 67). In the macaque study, the IL-12 DNA-adjuvanted vaccine groups showed enhanced magnitude and breadth of vaccine-induced immune responses.

In conclusion, our study describes a novel aspect of the post-translational regulation of IL-12p70 by its p40 subunit. These findings were applied for the generation of greatly improved IL-12 DNA plasmids expressing the two subunits in optimal configuration. These vectors could be useful for immunotherapy interventions against several types of cancer as well as viral infections, including AIDS.

*Acknowledgments—We thank J. Bear for technical assistance; M. Sidhu, M. A. Egan, and J. H. Eldridge for plasmids; and T. Jones for editorial assistance.*

## REFERENCES


1. Kobayashi, M., Fitz, L., Ryan, M., Hewick, R. M., Clark, S. C., Chan, S., Loudon, R., Sherman, F., Perussia, B., and Trinchieri, G. (1989) Identification and purification of natural killer cell stimulatory factor (NKSF), a cytokine with multiple biologic effects on human lymphocytes. *J. Exp. Med.* **170,** 827–845
2. Trinchieri, G., Wysocka, M., D'Andrea, A., Rengaraju, M., Aste-Amezaga, M., Kubin, M., Valiante, N. M., and Chehimi, J. (1992) Natural killer cell stimulatory factor (NKSF) or interleukin-12 is a key regulator of immune response and inflammation. *Prog. Growth Factor Res.* **4,** 355–368
3. Vignali, D. A., and Kuchroo, V. K. (2012) IL-12 family cytokines. Immunological playmakers. *Nat. Immunol.* **13,** 722–728
4. Lyakh, L., Trinchieri, G., Provezza, L., Carra, G., and Gerosa, F. (2008) Regulation of interleukin-12/interleukin-23 production and the T-helper 17 response in humans. *Immunol. Rev.* **226,** 112–131
5. Xu, M., Mizoguchi, I., Morishima, N., Chiba, Y., Mizuguchi, J., and Yoshimoto, T. (2010) Regulation of antitumor immune responses by the IL-12 family cytokines, IL-12, IL-23, and IL-27. *Clin. Dev. Immunol.* **2010**
6. Del Vecchio, M., Bajetta, E., Canova, S., Lotze, M. T., Wesa, A., Parmiani, G., and Anichini, A. (2007) Interleukin-12. Biological properties and clinical application. *Clin. Cancer Res.* **13,** 4677–4685
7. Weiss, J. M., Subleski, J. J., Wigginton, J. M., and Wiltrout, R. H. (2007) Immunotherapy of cancer by IL-12-based cytokine combinations. *Expert Opin. Biol. Ther.* **7,** 1705–1721
8. Villinger, F. (2003) Cytokines as clinical adjuvants. How far are we? *Expert Rev. Vaccines* **2,** 317–326
9. Sangro, B., Melero, I., Qian, C., and Prieto, J. (2005) Gene therapy of cancer based on interleukin 12. *Curr. Gene Ther.* **5,** 573–581
10. Portielje, J. E., Gratama, J. W., van Ojik, H. H., Stoter, G., and Kruit, W. H. (2003) IL-12. A promising adjuvant for cancer vaccination. *Cancer Immunol. Immunother.* **52,** 133–144
11. Waldner, M. J., and Neurath, M. F. (2009) Gene therapy using IL-12 family members in infection, auto immunity, and cancer. *Curr. Gene. Ther.* **9,** 239–247
12. Gubler, U., Chua, A. O., Schoenhaut, D. S., Dwyer, C. M., McComas, W., Motyka, R., Nabavi, N., Wolitzky, A. G., Quinn, P. M., and Familletti, P. C. (1991) Coexpression of two distinct genes is required to generate secreted bioactive cytotoxic lymphocyte maturation factor. *Proc. Natl. Acad. Sci. U.S.A.* **88,** 4143–4147
13. Wolf, S. F., Temple, P. A., Kobayashi, M., Young, D., Dicig, M., Lowe, L., Dzialo, R., Fitz, L., Ferenz, C., and Hewick, R. M. (1991) Cloning of cDNA for natural killer cell stimulatory factor, a heterodimeric cytokine with multiple biologic effects on T and natural killer cells. *J. Immunol.* **146,** 3074–3081
14. Schoenhaut, D. S., Chua, A. O., Wolitzky, A. G., Quinn, P. M., Dwyer, C. M., McComas, W., Familletti, P. C., Gately, M. K., and Gubler, U. (1992) Cloning and expression of murine IL-12. *J. Immunol.* **148,** 3433–3440
15. Trinchieri, G. (2003) Interleukin-12 and the regulation of innate resistance and adaptive immunity. *Nat. Rev. Immunol.* **3,** 133–146
16. Ling, P., Gately, M. K., Gubler, U., Stern, A. S., Lin, P., Hollfelder, K., Su, C., Pan, Y. C., and Hakimi, J. (1995) Human IL-12 p40 homodimer binds to the IL-12 receptor but does not mediate biologic activity. *J. Immunol.* **154,** 116–127
17. Gillessen, S., Carvajal, D., Ling, P., Podlaski, F. J., Stremlo, D. L., Familletti, P. C., Gubler, U., Presky, D. H., Stern, A. S., and Gately, M. K. (1995) Mouse interleukin-12 (IL-12) p40 homodimer. A potent IL-12 antagonist. *Eur. J. Immunol.* **25,** 200–206
18. Bergamaschi, C., Jalah, R., Kulkarni, V., Rosati, M., Zhang, G. M., Alicea, C., Zolotukhin, A. S., Felber, B. K., and Pavlakis, G. N. (2009) Secretion and biological activity of short signal peptide IL-15 is chaperoned by IL-15 receptor α *in vivo*. *J. Immunol.* **183,** 3064–3072
19. Bergamaschi, C., Rosati, M., Jalah, R., Valentin, A., Kulkarni, V., Alicea, C., Zhang, G. M., Patel, V., Felber, B. K., and Pavlakis, G. N. (2008) Intracellular interaction of interleukin-15 with its receptor α during production leads to mutual stabilization and increased bioactivity. *J. Biol. Chem.* **283,** 4189–4199
20. Bergamaschi, C., Bear, J., Rosati, M., Beach, R. K., Alicea, C., Sowder, R., Chertova, E., Rosenberg, S. A., Felber, B. K., and Pavlakis, G. N. (2012) Circulating interleukin-15 (IL-15) exists as heterodimeric complex with soluble IL-15 receptor α (IL-15Rα) in human serum. *Blood* **120,** e1–e8
21. Cole, D. J., and Rubinstein, M. P. (2012) Soluble IL-15/IL-15Rα complexes in human serum. *Blood* **120,** 1–2
22. Kalams, S. A., Parker, S., Jin, X., Elizaga, M., Metch, B., Wang, M., Hural, J., Lubeck, M., Eldridge, J., Cardinali, M., Blattner, W. A., Sobieszczyk, M., Suriyanon, V., Kalichman, A., Weiner, D. B., and Baden, L. R. (2012) Safety and immunogenicity of an HIV-1 gag DNA vaccine with or without IL-12 and/or IL-15 plasmid cytokine adjuvant in healthy, HIV-1 uninfected adults. *PLoS ONE* **7,** e29231
23. Egan, M. A., Megati, S., Roopchand, V., Garcia-Hand, D., Luckay, A., Chong, S. Y., Rosati, M., Sackitey, S., Weiner, D. B., Felber, B. K., Pavlakis, G. N., Israel, Z. R., Eldridge, J. H., and Sidhu, M. K. (2006) Rational design of a plasmid DNA vaccine capable of eliciting cell-mediated immune responses to multiple HIV antigens in mice. *Vaccine* **24,** 4510–4523
24. Schadeck, E. B., Sidhu, M., Egan, M. A., Chong, S.-Y., Piacente, P., Masood, A., Garcia-Hand, D., Cappello, S., Roopchand, V., Megati, S., Quiroz, J., Boyer, J. D., Felber, B. K., Pavlakis, G. N., Weiner, D. B., Eldridge, J. H., and Israel, Z. R. (2006) Plasmid encoded IL-12 functions as a DNA vaccine adjuvant and augments SIVgag-specific cell-mediated and humoral immune responses in Rhesus macaques. *Vaccine* **24,** 4677–4687
25. Nasioulas, G., Zolotukhin, A. S., Tabernero, C., Solomin, L., Cunningham, C. P., Pavlakis, G. N., and Felber, B. K. (1994) Elements distinct from human immunodeficiency virus type 1 splice sites are responsible for the Rev dependence of env mRNA. *J. Virol.* **68,** 2986–2993
26. Schwartz, S., Felber, B. K., and Pavlakis, G. N. (1992) Distinct RNA sequences in the gag region of human immunodeficiency virus type 1 decrease RNA stability and inhibit expression in the absence of Rev protein. *J. Virol.* **66,** 150–159
27. Schneider, R., Campbell, M., Nasioulas, G., Felber, B. K., and Pavlakis, G. N. (1997) Inactivation of the human immunodeficiency virus type 1 inhibitory elements allows Rev-independent expression of Gag and Gag/protease and particle formation. *J. Virol.* **71,** 4892–4903

28. Rosati, M., von Gegerfelt, A., Roth, P., Alicea, C., Valentin, A., Robert-Guroff, M., Venzon, D., Montefiori, D. C., Markham, P., Felber, B. K., and Pavlakis, G. N. (2005) DNA vaccines expressing different forms of simian immunodeficiency virus antigens decrease viremia upon SIVmac251 challenge. *J. Virol.* **79,** 8480–8492
29. Kulkarni, V., Jalah, R., Ganneru, B., Bergamaschi, C., Alicea, C., von Gegerfelt, A., Patel, V., Zhang, G. M., Chowdhury, B., Broderick, K. E., Sardesai, N. Y., Valentin, A., Rosati, M., Felber, B. K., and Pavlakis, G. N. (2011) Comparison of immune responses generated by optimized DNA vaccination against SIV antigens in mice and macaques. *Vaccine* **29,** 6742–6754
30. Jalah, R., Rosati, M., Kulkarni, V., Patel, V., Bergamaschi, C., Valentin, A., Zhang, G. M., Sidhu, M. K., Eldridge, J. H., Weiner, D. B., Pavlakis, G. N., and Felber, B. K. (2007) Efficient systemic expression of bioactive IL-15 in mice upon delivery of optimized DNA expression plasmids. *DNA Cell Biol.* **26,** 827–840
31. Egan, M. A., Chong, S. Y., Megati, S., Montefiori, D. C., Rose, N. F., Boyer, J. D., Sidhu, M. K., Quiroz, J., Rosati, M., Schadeck, E. B., Pavlakis, G. N., Weiner, D. B., Rose, J. K., Israel, Z. R., Udem, S. A., and Eldridge, J. H. (2005) Priming with plasmid DNAs expressing interleukin-12 and simian immunodeficiency virus gag enhances the immunogenicity and efficacy of an experimental AIDS vaccine based on recombinant vesicular stomatitis virus. *AIDS Res. Hum. Retroviruses* **21,** 629–643
32. Stauber, R., Gaitanaris, G. A., and Pavlakis, G. N. (1995) Analysis of trafficking of Rev and transdominant Rev proteins in living cells using green fluorescent protein fusions. Transdominant Rev blocks the export of Rev from the nucleus to the cytoplasm. *Virology* **213,** 439–449
33. Schwartz, S., Felber, B. K., Benko, D. M., Fenyö, E. M., and Pavlakis, G. N. (1990) Cloning and functional analysis of multiply spliced mRNA species of human immunodeficiency virus type 1. *J. Virol.* **64,** 2519–2529
34. Ortaldo, J. R., Winkler-Pickett, R. T., Bere, E. W., Jr., Watanabe, M., Murphy, W. J., and Wiltrout, R. H. (2005) *In vivo* hydrodynamic delivery of cDNA encoding IL-2. Rapid, sustained redistribution, activation of mouse NK cells, and therapeutic potential in the absence of NKT cells. *J. Immunol.* **175,** 693–699
35. Jiang, J., Yamato, E., and Miyazaki, J. (2001) Intravenous delivery of naked plasmid DNA for *in vivo* cytokine expression. *Biochem. Biophys. Res. Commun.* **289,** 1088–1092
36. Liu, F., Song, Y., and Liu, D. (1999) Hydrodynamics-based transfection in animals by systemic administration of plasmid DNA. *Gene. Ther.* **6,** 1258–1266
37. Schwartz, S., Campbell, M., Nasioulas, G., Harrison, J., Felber, B. K., and Pavlakis, G. N. (1992) Mutational inactivation of an inhibitory sequence in human immunodeficiency virus type 1 results in Rev-independent gag expression. *J. Virol.* **66,** 7176–7182
38. Carra, G., Gerosa, F., and Trinchieri, G. (2000) Biosynthesis and posttranslational regulation of human IL-12. *J. Immunol.* **164,** 4752–4761
39. Murphy, F. J., Hayes, M. P., and Burd, P. R. (2000) Disparate intracellular processing of human IL-12 preprotein subunits. Atypical processing of the p35 signal peptide. *J. Immunol.* **164,** 839–847
40. Heinzel, F. P., Hujer, A. M., Ahmed, F. N., and Rerko, R. M. (1997) *In vivo* production and function of IL-12 p40 homodimers. *J. Immunol.* **158,** 4381–4388
41. Mattner, F., Fischer, S., Guckes, S., Jin, S., Kaulen, H., Schmitt, E., Rüde, E., and Germann, T. (1993) The interleukin-12 subunit p40 specifically inhibits effects of the interleukin-12 heterodimer. *Eur. J. Immunol.* **23,** 2202–2208
42. Vaidyanathan, H., Zhou, Y., Petro, T. M., and Schwartzbach, S. D. (2003) Intracellular localization of the p35 subunit of murine IL-12. *Cytokine* **21,** 120–128
43. Jalah, R., Patel, V., Kulkarni, V., Rosati, M., Alicea, C., Ganneru, B., von Gegerfelt, A., Huang, W., Guan, Y., Broderick, K. E., Sardesai, N. Y., Labranche, C., Montefiori, D. C., Pavlakis, G. N., and Felber, B. K. (2012) IL-12 DNA as molecular vaccine adjuvant increases the cytotoxic T cell responses and breadth of humoral immune responses in SIV DNA vaccinated macaques. *Hum. Vaccin. Immunother.* **8,** 1620–1629
44. Chong, S. Y., Egan, M. A., Kutzler, M. A., Megati, S., Masood, A., Roopchard, V., Garcia-Hand, D., Montefiori, D. C., Quiroz, J., Rosati, M., Schadeck, E. B., Boyer, J. D., Pavlakis, G. N., Weiner, D. B., Sidhu, M., Eldridge, J. H., and Israel, Z. R. (2007) Comparative ability of plasmid IL-12 and IL-15 to enhance cellular and humoral immune responses elicited by a SIVgag plasmid DNA vaccine and alter disease progression following SHIV(89.6P) challenge in rhesus macaques. *Vaccine* **25,** 4967–4982
45. Boyer, J. D., Robinson, T. M., Kutzler, M. A., Parkinson, R., Calarota, S. A., Sidhu, M. K., Muthumani, K., Lewis, M., Pavlakis, G., Felber, B., and Weiner, D. (2005) SIV DNA vaccine co-administered with IL-12 expression plasmid enhances CD8 SIV cellular immune responses in cynomolgus macaques. *J. Med. Primatol.* **34,** 262–270
46. Gee, K., Guzzo, C., Che Mat, N. F., Ma, W., and Kumar, A. (2009) The IL-12 family of cytokines in infection, inflammation and autoimmune disorders. *Inflamm. Allergy Drug Targets* **8,** 40–52
47. Goriely, S., and Goldman, M. (2008) Interleukin-12 family members and the balance between rejection and tolerance. *Curr. Opin. Organ Transplant.* **13,** 4–9
48. Snijders, A., Hilkens, C. M., van der Pouw Kraan, T. C., Engel, M., Aarden, L. A., and Kapsenberg, M. L. (1996) Regulation of bioactive IL-12 production in lipopolysaccharide-stimulated human monocytes is determined by the expression of the p35 subunit. *J. Immunol.* **156,** 1207–1212
49. Liu, W., Wei, H., Liang, S., Zhang, J., Sun, R., and Tian, Z. (2004) A balanced expression of two chains of heterodimer protein, the human interleukin-12, improves high-level expression of the protein in CHO cells. *Biochem. Biophys. Res. Commun.* **313,** 287–293
50. D'Andrea, A., Rengaraju, M., Valiante, N. M., Chehimi, J., Kubin, M., Aste, M., Chan, S. H., Kobayashi, M., Young, D., and Nickbarg, E. (1992) Production of natural killer cell stimulatory factor (interleukin 12) by peripheral blood mononuclear cells. *J. Exp. Med.* **176,** 1387–1398
51. Cassatella, M. A., Meda, L., Gasperini, S., D'Andrea, A., Ma, X., and Trinchieri, G. (1995) Interleukin-12 production by human polymorphonuclear leukocytes. *Eur. J. Immunol.* **25,** 1–5
52. Duitman, E. H., Orinska, Z., and Bulfone-Paus, S. (2011) Mechanisms of cytokine secretion. A portfolio of distinct pathways allows flexibility in cytokine activity. *Eur. J. Cell Biol.* **90,** 476–483
53. Duitman, E. H., Orinska, Z., Bulanova, E., Paus, R., and Bulfone-Paus, S. (2008) How a cytokine is chaperoned through the secretory pathway by complexing with its own receptor. Lessons from interleukin-15 (IL-15)/IL-15 receptor α. *Mol. Cell Biol.* **28,** 4851–4861
54. Mortier, E., Woo, T., Advincula, R., Gozalo, S., and Ma, A. (2008) IL-15Rα chaperones IL-15 to stable dendritic cell membrane complexes that activate NK cells via trans presentation. *J. Exp. Med.* **205,** 1213–1225
55. Rubinstein, M. P., Kovar, M., Purton, J. F., Cho, J. H., Boyman, O., Surh, C. D., and Sprent, J. (2006) Converting IL-15 to a superagonist by binding to soluble IL-15Rα. *Proc. Natl. Acad. Sci. U.S.A.* **103,** 9166–9171
56. Babik, J. M., Adams, E., Tone, Y., Fairchild, P. J., Tone, M., and Waldmann, H. (1999) Expression of murine IL-12 is regulated by translational control of the p35 subunit. *J. Immunol.* **162,** 4069–4078
57. Tagaya, Y., Kurys, G., Thies, T. A., Losi, J. M., Azimi, N., Hanover, J. A., Bamford, R. N., and Waldmann, T. A. (1997) Generation of secretable and nonsecretable interleukin 15 isoforms through alternate usage of signal peptides. *Proc. Natl. Acad. Sci. U.S.A.* **94,** 14444–14449
58. Zhang, L., Kerkar, S. P., Yu, Z., Zheng, Z., Yang, S., Restifo, N. P., Rosenberg, S. A., and Morgan, R. A. (2011) Improving adoptive T cell therapy by targeting and controlling IL-12 expression to the tumor environment. *Mol. Ther.* **19,** 751–759
59. Mahvi, D. M., Henry, M. B., Albertini, M. R., Weber, S., Meredith, K., Schalch, H., Rakhmilevich, A., Hank, J., and Sondel, P. (2007) Intratumoral injection of IL-12 plasmid DNA. Results of a phase I/IB clinical trial. *Cancer Gene Ther.* **14,** 717–723
60. Anwer, K., Barnes, M. N., Fewell, J., Lewis, D. H., and Alvarez, R. D. (2010) Phase-I clinical trial of IL-12 plasmid/lipopolymer complexes for the treatment of recurrent ovarian cancer. *Gene. Ther.* **17,** 360–369
61. Heinzerling, L., Burg, G., Dummer, R., Maier, T., Oberholzer, P. A., Schultz, J., Elzaouk, L., Pavlovic, J., and Moelling, K. (2005) Intratumoral injection of DNA encoding human interleukin 12 into patients with metastatic melanoma. Clinical efficacy. *Hum. Gene Ther.* **16,** 35–48
62. Daud, A. I., DeConti, R. C., Andrews, S., Urbas, P., Riker, A. I., Sondak, V. K., Munster, P. N., Sullivan, D. M., Ugen, K. E., Messina, J. L., and Heller,

R. (2008) Phase I trial of interleukin-12 plasmid electroporation in patients with metastatic melanoma. *J. Clin. Oncol.* **26,** 5896–5903
63. Heller, L. C., and Heller, R. (2010) Electroporation gene therapy preclinical and clinical trials for melanoma. *Curr. Gene. Ther.* **10,** 312–317
64. Heller, R., Schultz, J., Lucas, M. L., Jaroszeski, M. J., Heller, L. C., Gilbert, R. A., Moelling, K., and Nicolau, C. (2001) Intradermal delivery of interleukin-12 plasmid DNA by *in vivo* electroporation. *DNA Cell Biol.* **20,** 21–26
65. Kerkar, S. P., Goldszmid, R. S., Muranski, P., Chinnasamy, D., Yu, Z., Reger, R. N., Leonardi, A. J., Morgan, R. A., Wang, E., Marincola, F. M., Trinchieri, G., Rosenberg, S. A., and Restifo, N. P. (2011) IL-12 triggers a programmatic change in dysfunctional myeloid-derived cells within mouse tumors. *J. Clin. Invest.* **121,** 4746–4757
66. Whitworth, J. M., and Alvarez, R. D. (2011) Evaluating the role of IL-12 based therapies in ovarian cancer. A review of the literature. *Expert. Opin. Biol. Ther.* **11,** 751–762
67. Winstone, N., Wilson, A. J., Morrow, G., Boggiano, C., Chiuchiolo, M. J., Lopez, M., Kemelman, M., Ginsberg, A. A., Mullen, K., Coleman, J. W., Wu, C. D., Narpala, S., Ouellette, I., Dean, H. J., Lin, F., Sardesai, N. Y., Cassamasa, H., McBride, D., Felber, B. K., Pavlakis, G. N., Schultz, A., Hudgens, M. G., King, C. R., Zamb, T. J., Parks, C. L., and McDermott, A. B. (2011) Enhanced control of pathogenic SIVmac239 replication in macaques immunized with a plasmid IL12 and a DNA prime, viral vector boost vaccine regimen. *J. Virol.* **85,** 9578–9587
68. Lieschke, G. J., Rao, P. K., Gately, M. K., and Mulligan, R. C. (1997) Bioactive murine and human interleukin-12 fusion proteins which retain antitumor activity *in vivo*. *Nat. Biotechnol.* **15,** 35–40
69. Anderson, R., Macdonald, I., Corbett, T., Hacking, G., Lowdell, M. W., and Prentice, H. G. (1997) Construction and biological characterization of an interleukin-12 fusion protein (Flexi-12). Delivery to acute myeloid leukemic blasts using adeno-associated virus. *Hum. Gene Ther.* **8,** 1125–1135